Numerical and semi-analytical solutions of the compound layer growth kinetics in cylindrical surfaces during plasma nitriding of pure iron

Numerical and semi-analytical solutions of the compound layer growth kinetics in cylindrical surfaces during plasma nitriding of pure iron

E M Hernández, F Castillo, R D Santiago, R Martínez, J A Otero, J E Oseguera and A Jiménez

Tecnológico de Monterrey, Campus Estado de México, Atizapán de Zaragoza, 52926 Edo. de Mex., Mexico.

E-mail: francast@itesm.mx

Abstract. Numerical and approximate analytical solutions for the compact layer growth kinetics in a pure iron solid cylinder, during a plasma nitriding process, are obtained. The numerical simulations of the model are performed by using a front tracking finite difference scheme and the heat balance integral method. We propose a model where the main assumption is to consider a diffusion zone of constant thickness, which is solved for cylindrical symmetries. We present results for the time evolution of the compound layer, where the obtained solutions from both methods are consistent with the expected behaviour in the asymptotic time limit and experimental data from other authors.

1. Introduction

Nitriding thermochemical treatments in different kind of steels are broadly used in industry because of their numerous applications [1, 2]. Nitriding can be performed with gas containing ammonia or cyanide salts and also through weakly ionized plasma [3]. The nitrogen flux from the surface into the bulk, carries allotropic transformations, which notably enhance the mechanical and chemical properties of piece. The combination of a compact nitride layer, followed by a diffusion zone in ferrite, produces an important improvement in wear resistance, a significant increase in hardness and in many cases, progression of fatigue resistance. Plasma assisted thermochemical treatments allow diffusion to occur at low temperatures compared to other processes [1-3], so that very low distortions are developed in pieces. In addition, these treatments produce no pollutants.

Modeling the concomitant growth of compact layers of nitrides in the Fe-N_2 thermodynamic system has been targeted by several authors [4-7]. An important aspect of the mathematical modelling of nitriding processes, is the geometry of the piece under treatment [8, 9]. Many papers are devoted only to the modeling of layer growth kinetics over plane surfaces; therefore, this work is focused on the study of nitride layer growth on cylindrical symmetries. Considering mass balance at each interface, we have performed a numerical simulation for the concomitant growth of compact nitride layers during plasma nitriding within a solid cylinder of pure iron. We will show that for these kind of geometries, the solutions obtained from the finite difference scheme (FDS) and heat balance integral method (HBIM), are able to capture the physical behavior of the process.

2. Problem statement

2.1 Mathematical model

We will consider an iron sample with a cylindrical cross section where nitrogen gas has penetrated in such a way that at time t_0, the ε, γ' and α phases are already formed. The surface concentration is constant and equal to $C_\varepsilon^{\max}$ and the boundary conditions at each interface are determined through the Fe-N_2 phase diagram. The surface concentration of nitrogen located at $x=R$ is denoted as $C_\varepsilon^{\max}$, where R is the radius of the sample. Therefore, the boundary conditions in cylindrical coordinates are given by

$$C_1(R,t)=C_\varepsilon^{\max},\ C_1(R-\xi_\varepsilon,t)=C_\varepsilon^{\min}, \tag{1}$$

at the ε phase, where ξ_ε is the thickness of the ε layer. Furthermore, with $\xi_{\gamma'}$ and ξ_α defined as the γ' and diffusion zone thicknesses respectively, the boundary conditions for each layer are given by

$$C_2(R-\xi_\varepsilon,t)=C_{\gamma'}^{\max},\ C_2(R-\xi_\varepsilon-\xi_{\gamma'},t)=C_{\gamma'}^{\min}, \tag{2}$$

and

$$C_3(R-\xi_\varepsilon-\xi_{\gamma'},t)=C_\alpha^{\max},\ C_3(R-\xi_\varepsilon-\xi_{\gamma'}-\xi_\alpha,t)=C_\alpha^{\min}. \tag{3}$$

Nitrogen transport within iron is assumed to be of Fickian nature. Consequently, classical diffusion equations are used to describe mass transport phenomena, and due to the symmetry of the system, the diffusion equations are solved in cylindrical coordinates. Interface motion is driven by the flux jump through the following Stefan condition

$$\bar{C}_{i,i+1}\frac{dL_i}{dt}=D_{i+1}\frac{\partial C_{i+1}(x,t)}{\partial x}\Big|_{x=L_i}-D_i\frac{\partial C_i(x,t)}{\partial x}\Big|_{x=L_i},\ i=1,2 \tag{4}$$

where the constants $\bar{C}_{i,i+1}$ represent the concentration jump at each interface, in such a way that for $i=1$, $\bar{C}_{1,2}=C_\varepsilon^{\min}-C_{\gamma'}^{\max}$, $D_1=D_\varepsilon$ and $D_2=D_{\gamma'}$. For $i=2$, $\bar{C}_{2,3}=C_{\gamma'}^{\min}-C_\alpha^{\max}$ and $D_3=D_\alpha$. Moreover, for $i=1$, L_i represents the epsilon layer thickness, as $L_1=\xi_\varepsilon$; for $i=2$, L_i represents the compound layer thickness $L_2=\xi_\varepsilon+\xi_{\gamma'}$, and for $i=3$, L_i represents the compound layer and diffusion zone widths $L_3=\xi_\varepsilon+\xi_{\gamma'}+\xi_\alpha$. The main idea of this proposal, is the assumption of a diffusion zone with constant thickness. Based on this assumption, the kinetics of the interface between the α zone and pure iron matrix is only governed by the motion of the ε/γ' and γ'/α interfaces. As a result of this, the diffusion zone is being pushed by the compound layer.

2.2 Numerical solutions

A second order FDS and the HBIM are used to solve the diffusion equations, along with the Stefan condition at the ε/γ' and γ'/α interfaces given by equation (4). In order to obtain a physically viable solution from the HBIM, we test the type of concentration profiles that have been proposed for cylindrical configurations in heat conduction problems [11], such as a linear-log and parabolic-log profile. The initial parabolic profiles used to solve the diffusion equations and the Stefan condition are given by

$$C_i(x,t)=C_i^{\min}+a_i(t)(R-L_i-x)+b_i(t)\ln\left(\frac{x}{R-L_i}\right), \tag{5}$$

for $i=1,2$. Finally, the proposed concentration profile for the diffusion zone is written as

$$C_3(x,t) = C_\alpha^{\max} + a_3(t)(R - L_2 - x) + b_3(t)\ln\left(\frac{x}{R-L_2}\right) \tag{6}$$

The initial concentration profiles are obtained by calculating the functions $b_i(t)$ from the boundary conditions described in section 2.1, and assuming an initial logarithmic profile. It was shown in [10] that for this model, the concentration profile is linear for large time values, and does not depend on the shape of the initial profile. It will be shown here, that for a cylindrical geometry this holds as well.

3. Results and Discussion

The results obtained with the FDS and the HBIM described in section 2 will be shown in this section. For the numerical simulations, the nitriding temperature used is $793\,\mathrm{K}$, effective diffusion constants at each layer are $D_\varepsilon = 5.3367\times10^{-15}\,\mathrm{m^2/s}$, $D_{\gamma'} = 5.8555\times10^{-14}\,\mathrm{m^2/s}$ and $D_\alpha = 4.9343\times10^{-12}\,\mathrm{m^2/s}$. The concentrations at each interface are taken from the Fe-N_2 phase diagram as $C_\varepsilon^{\max} = 7.68$, $C_\varepsilon^{\min} = 7.5204$, $C_{\gamma'}^{\max} = 5.8849$, $C_{\gamma'}^{\min} = 5.7738$, $C_\alpha^{\max} = 0.0627$ and $C_\alpha^{\min} = 0.0$ in % wt. Finally, the initial thickness of each layer is assumed to be $\xi_\varepsilon = 0.0480\,\mu\mathrm{m}$, $\xi_{\gamma'} = 0.3739\,\mu\mathrm{m}$ and $\xi_\alpha = 80\,\mu\mathrm{m}$, as in [10].

All figures below, show the results obtained for each layer, by using the FDS and HBIM described in section 2. In figure 1, we show the solutions from both methods for a sample of radius $R = 0.10$ m and a diffusion zone $80\,\mu\mathrm{m}$ thick. An important consequence of this model is that for large time values, the jump in the net flux through each interface approaches zero; therefore

$$D_\varepsilon(C_\varepsilon^{\max} - C_\varepsilon^{\min})/\xi_\varepsilon = D_{\gamma'}(C_{\gamma'}^{\max} - C_{\gamma'}^{\min})/\xi_{\gamma'}, \qquad D_{\gamma'}(C_{\gamma'}^{\max} - C_{\gamma'}^{\min})/\xi_{\gamma'} = D_\alpha(C_\alpha^{\max} - C_\alpha^{\min})/\xi_\alpha. \tag{7}$$

From equation (7) it is easy to obtain the thickness of each layer in the asymptotic time limit [10], as

$$\xi_{\gamma'\text{-lim}} = \frac{D_{\gamma'}\left(C_{\gamma'}^{\max} - C_{\gamma'}^{\min}\right)}{D_\alpha\left(C_\alpha^{\max} - C_\alpha^{\min}\right)}\xi_\alpha, \qquad \xi_{\varepsilon\text{-lim}} = \frac{D_\varepsilon\left(C_\varepsilon^{\max} - C_\varepsilon^{\min}\right)}{D_{\gamma'}\left(C_{\gamma'}^{\max} - C_{\gamma'}^{\min}\right)}\xi_{\gamma'\text{-lim}}. \tag{8}$$

In this time limit, the net flux of mass through a point x within any layer is zero; therefore

$$\frac{D_i\left(C_i^{\max} - C_i(x)\right)}{R - x - L_{\text{i-1}}} = \frac{D_i\left(C_i(x) - C_i^{\min}\right)}{x - (R - L_{\text{i}})},$$

which can be solved for the concentration at an arbitrary point within the compound layer or diffusion zone as

$$C_i(x) = \frac{C_i^{\max} - C_i^{\min}}{(L_i - L_{i-1})}(x - R) + \frac{C_i^{\max}L_i - C_i^{\min}L_{i-1}}{(L_i - L_{i-1})}, \text{ for } R - L_i < x < R - L_{i-1} \tag{9}$$

On each figure we use equation (8) to check that every solution obtained through any of the proposed methods, captures the predicted behaviour for large time values. In figures 2 and 3 the results for several values of the sample radius are shown and compared against the predicted thickness of each layer, in the asymptotic time limit. In figure 2, the results from the FDS and HBIM are shown for the ε layer. As can be observed, there is a weak dependence on the radius of the sample.

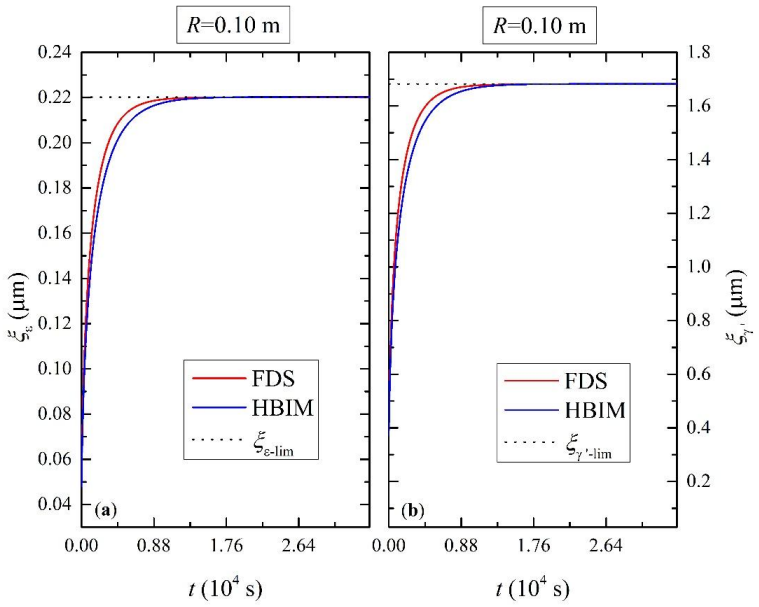

Figure 1. FDS and HBIM solutions for the time evolution of the ε and γ' layer thicknesses.

Finally, similar results for the γ' layer growth kinetics are shown in figure 3. Also in this case, the solutions obtained from the FDS and HBIM, do not depend significantly on the radius of the sample.

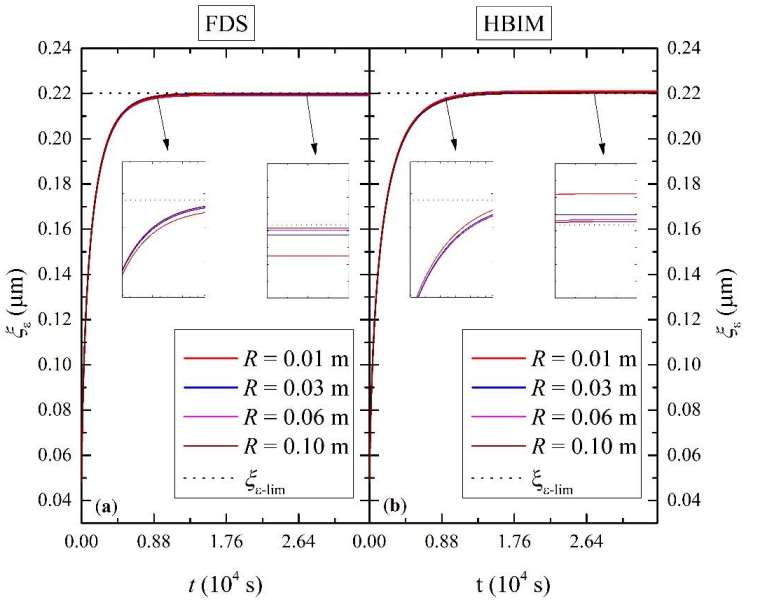

Figure 2. Time evolution of the ε layer for different values of the sample radius. a) FDS and b) HBIM solutions for a diffusion zone of $80\,\mu$m.

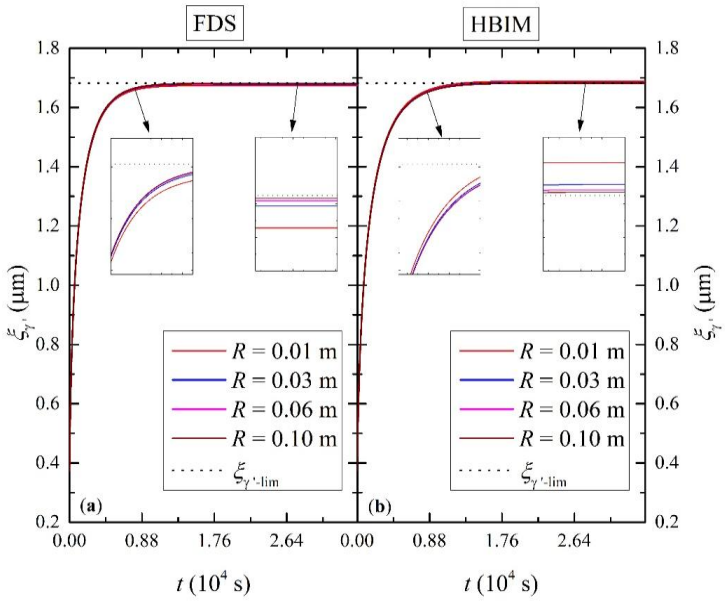

Figure 3. a) FDS and b) HBIM solutions for γ' layer growth with different values of R.

A comparison between the experimental results of [4] which are performed on planar samples and the solutions obtained for a cylindrical geometry is shown in figure 4. Each curve belongs to the solution calculated for a specific thickness of the diffusion zone. As the width of ξ_α is increased, the relative difference between adjacent curves reduces monotonically. The largest value of ξ_α belongs to the continuous line, which is shown in figure 4. For this value, the asymptotic limit is reached at $t \approx 2\times10^{10}\,\mathrm{s}$, which is 10^6 orders of magnitude larger than the total nitriding time used in the experiment of [4]. For this reason, further increase in ξ_α, produces almost identical results to the curves shown in solid lines, which correspond to the solutions used to compare with the experimental data. These numerical experiments suggest a constant thickness of the diffusion layer. Solutions of this model were obtained for planar geometries [10], which are very close to the numerical solutions obtained here for cylindrical geometries.

For small values of ξ_α, the mass flux through the diffusion zone is of the same order of magnitude than the flux through the γ' layer, which implies that α iron is quickly saturated with Nitrogen, slowing any further growth of the γ' layer. This is illustrated in figure 4, where the dashed line corresponding to the smallest value of ξ_α is observed to approach very rapidly to the asymptotic limit. In fact, once the compound layer has formed, diffusion zones are typically several orders of magnitude thicker than ε and γ' layers, because effective diffusion coefficients for the diffusion zone are two orders of magnitude larger than those corresponding to ε and γ' layers. Thus, for typical values of ξ_α, the flux through this zone is very small compared to the flux within the γ' layer, this is why the influence of mass transport within the diffusion zone is almost negligible. By considering a large diffusion zone of constant thickness, the proposed model is neglecting the effects that mass transport within the diffusion zone may have on the compound layer growth kinetics. This is shown to be a good approximation, once each layer is formed. Therefore, in order to compare the results from the proposed model, the starting point is chosen at time values where the diffusion zone is at least one order of magnitude thicker than any layer. For example, the numerical results shown in figure 4, are obtained by starting at $t = 3001.22\,\mathrm{s}$, where the first data point is reported in [4] and every layer is already formed.

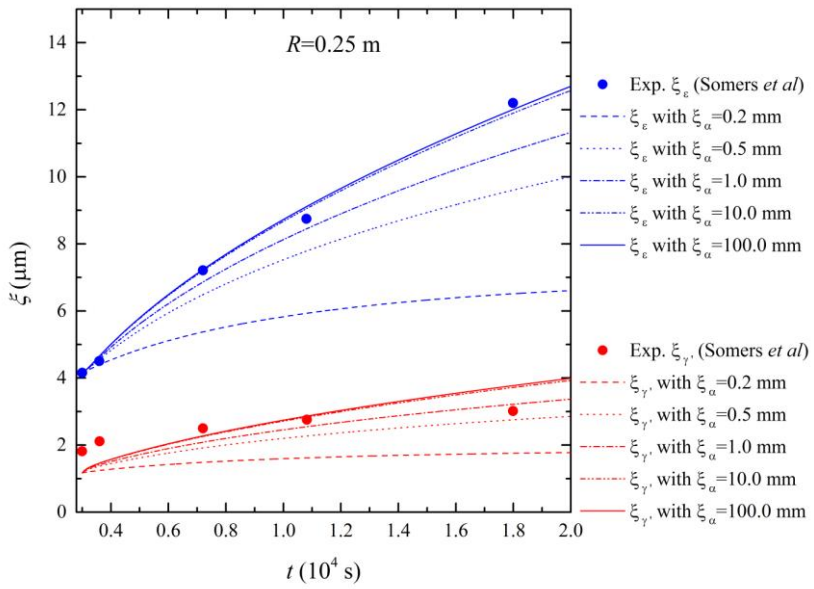

Figure 4 Solid lines correspond to the solutions obtained with the HBIM and data points from the experiment in [4] are shown in blue and red circles for each layer. The maximum relative difference between the numerical results and the experimental data is observed to be of 6.32%.

4. Conclusion

This work presents a correctly stated mathematical model of growth kinetics for compact concomitant layers of nitrides during plasma nitriding of pure iron in cylindrical surfaces. The introduced model is consistent with the mechanism of mass transfer (Fick's Second Law and mass balance at the interfaces) and relevant available information on the problem (diffusion coefficients and nitrogen solubility limits). The obtained solutions, employing data from other authors and information produced in our analysis, yield congruent results between the numerical and semi-analytical methods. Finally, our solutions are observed to be in excellent agreement with the values predicted by equation (8), and no significant dependence on the shape of the sample is observed, as can be expected from the predicted thickness of each layer, in the asymptotic time limit.

5. References

[1] Pye D 2003 *Practical Nitriding and Ferritic Nitrocarburizing* (ASM International Materials Park, Ohio)
[2] Bell T et al 1977 *Controlled Nitriding in Ammonia-Hydrogen Mixtures* (Source Book on Nitriding, American Society for Metals)
[3] Totten G E 2004 *Steel Heat Treatment: Metalurgy and Technologies* (CRC Press, Boca Raton)
[4] Somers M A J and Mittemeijer E J 1995 *Metall. Mater. Trans. A*, **26A** p 57
[5] Jaoul C, Belmonte T, Czerwiec T, Ablitzer D, Ricard A and Mitchell H 2006 *Thin Solid Films* **163** 506
[6] Christiansen T, Dahl K V and Somers M A J 2008 *Mater. Sci. Tech.* **24** p 159
[7] Marciniak A 1985 *Surface Eng.* **1** p 283
[8] Henry J, Topolsky J and Abramczuk M 1992 *Crankshaft Durability Prediction- A new 3-D Approach* (SAE Technical Paper No. 920087)
[9] Zoroufi M and Fatemi A 2005 *A literature review on durability evaluation of cranksshafts including comparison of competing manufacturing processes and costs analysis* (Proceedings of the 26th Forging Industry Technical Conference, Chicago)
[10] Hernandez E, Jimenez A, Otero J A, Santiago R D, Martinez R, Castillo F and Oseguera J 2016 *Sci. Res. Essays* **11(13)** pp 135-146
[11] Driscoll R J 2010 *Convective and Radiative Heat Transfer in a Thick Cylinder Using the Heat Balance Integral Method* (46th AIAA/ASME/SAE/ASEE Joint Propulsion Conference and Exhibit, Nashville)